STAR Protocols

CellPress
OPEN ACCESS

Protocol

Protocol to develop a preclinical severe contusive-compressive SCI mouse model for translational research

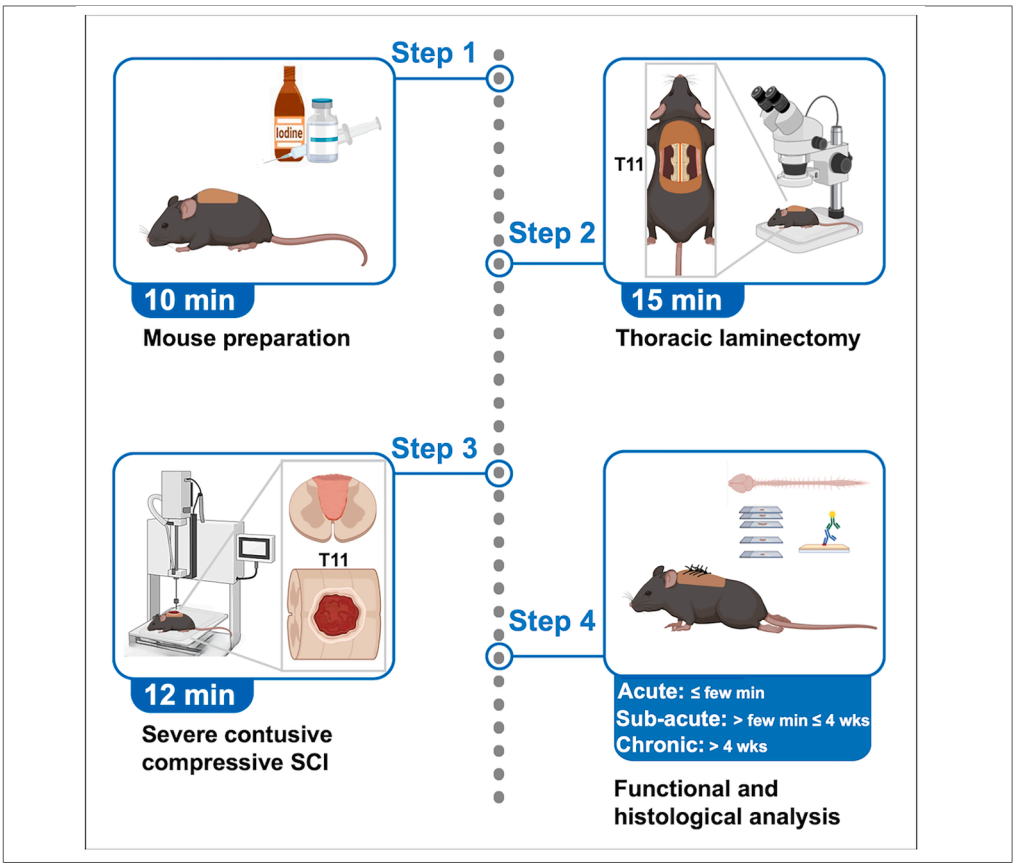

Complete spinal cord injury (SCI) leads to irreversible neurological damage due to failed neural repair, with no effective therapies currently available. Here, we present a protocol to induce severe contusive-compressive SCI at thoracic T11 level in mouse using the NYU-MASCIS II impactor. We describe steps for performing laminectomy, inducing the injury, and validating it through functional and histological analysis. This protocol replicates key aspects of human secondary injury, making it valuable for preclinical testing of SCI therapies.

Publisher's note: Undertaking any experimental protocol requires adherence to local institutional guidelines for laboratory safety and ethics.

Sissi Dolci, Marzia Di Chio, Giuseppe Busetto, Francesco Bifari, Ilaria Decimo

sissi.dolci@univr.it (S.D.)
ilaria.decimo@univr.it (I.D.)

Highlights

Instructions for performing surgery to expose the T11 thoracic spinal segment

Steps for inducing severe contusive-compressive SCI

Guidance on evaluating the functional motor recovery

Procedures for histological analysis of tissue alterations after SCI

Dolci et al., STAR Protocols 7, 104029
March 20, 2026
https://doi.org/10.1016/j.xpro.2025.104029

STAR Protocols

CellPress
OPEN ACCESS

Protocol

Protocol to develop a preclinical severe contusive-compressive SCI mouse model for translational research

Sissi Dolci,[1,4,*] Marzia Di Chio,[1] Giuseppe Busetto,[2] Francesco Bifari,[3] and Ilaria Decimo[1,5,*]

[1]Laboratory of Pharmacology, Department of Diagnostic and Public Health, University of Verona, 37134 Verona, Italy

[2]Department of Neuroscience Biomedicine and Movement Science, University of Verona, Verona, Italy

[3]Laboratory of Cell Metabolism and Regenerative Medicine, Department of Medical Biotechnology and Translational Medicine, University of Milan, Milan, Italy

[4]Technical contact

[5]Lead contact

*Correspondence: sissi.dolci@univr.it (S.D.), ilaria.decimo@univr.it (I.D.)
https://doi.org/10.1016/j.xpro.2025.104029

SUMMARY

Complete spinal cord injury (SCI) leads to irreversible neurological damage due to failed neural repair, with no effective therapies currently available. Here, we present a protocol to induce severe contusive-compressive SCI at thoracic T11 level in mouse using the NYU-MASCIS II impactor. We describe steps for performing laminectomy, inducing the injury, and validating it through functional and histological analysis. This protocol replicates key aspects of human secondary injury, making it valuable for preclinical testing of SCI therapies.

BEFORE YOU BEGIN

Innovation

The adult mammalian central nervous system (CNS) exhibits an ineffective wound repair process.[1] Despite most human SCI results from contusive-compressive trauma, animal models primarily focus on traumatic injuries, which do not accurately represent human conditions.[2–4] To address this gap, we developed and validated the first preclinical mouse model of severe contusive-compressive spinal cord injury (SCI), capable of replicating the pathophysiological features of human SCI that significantly affects the quality of life.[5–9] The severity of the injury was defined based on established parameters (5 grams rod dropped from 6.25 mm), previously shown to induce severe SCI in mice,[10–12] and further enhanced by an 11 seconds compression phase.[5] Based on our NYU parameters (5 grams weight and 6.25 mm drop height and 11 seconds compression), we calculated the corresponding impact force, which resulted in 61.3 KDyne (E = mgh = 0.005·9.81·0.00625=0.00030656J ≈0.31 mJ; F = 0.00030656 / 0.0005 = 0.613N = 61.3 KDyne; displacement value of 0.5 mm[13,14]). Unlike other rodent SCI models, that recover spontaneously after SCI,[15] this clinically relevant model leads to a permanent complete paralysis of the hindlimbs and severe impairment of bladder function,[5] consistent with outcomes seen in severe Infinity Horizon impactor-based models.[16,17] Here we describe the specific steps to obtain severe contusive-compressive SCI in mouse at T11 vertebra level. However, it can be used to deliver a severe impact at cervical and lumbar spinal cord levels on the base of the research interests.

Institutional permissions

All procedures on mice were approved by the National Institute of Health (protocol N.154/2014-B, Italy) and by the Animal Ethics Committee of the University of Verona (CIRSAL, Centro Interdipartimentale di Servizio alla Ricerca Sperimentale).

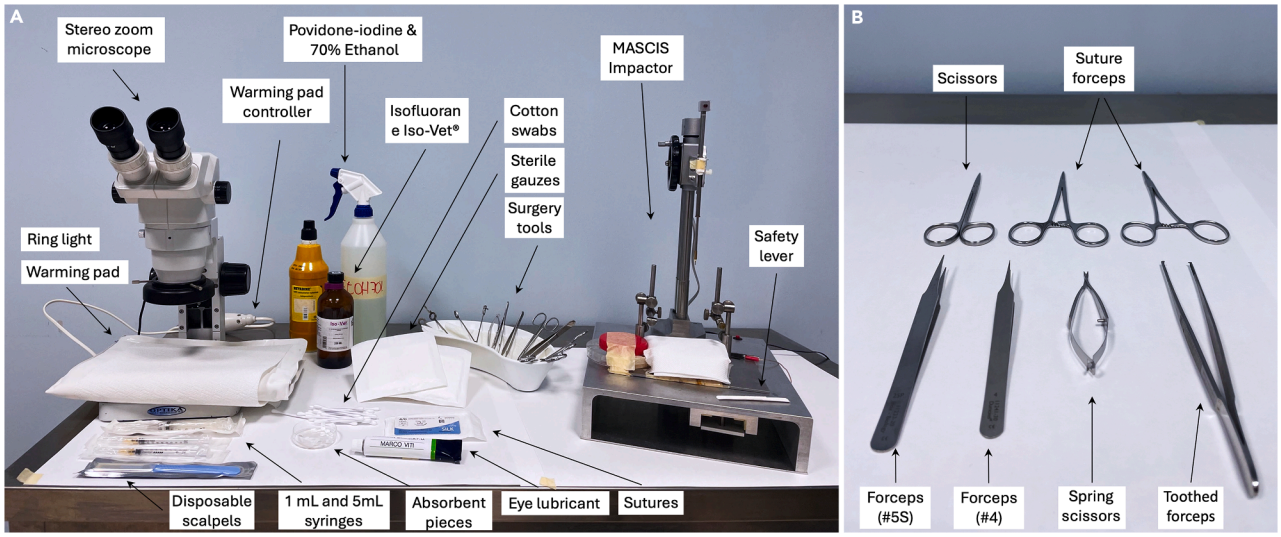

Figure 1. General surgery setup

(A) Material necessary for the severe contusive-compressive SCI.

(B) Surgery tools.

⚠ CRITICAL: Any experiments on live vertebrates or higher invertebrates must be performed in accordance with relevant institutional and national guidelines and regulations. Users are reminded that they will need to acquire the necessary animal permissions from the relevant institutions.

Mice shaving for the severe contusive-compressive SCI surgery

Timing: 3 min/mouse

1. The day before the injury surgery, place the mouse in a clean cage.
   a. Using an electric hair clipper/trimmer, shave the area around the hump at the middle back to remove any hair that might otherwise contaminate the surgical wound.
   b. Using a wet paper towel, gently wipe the shaved area to remove any loose hair that may have settled on the skin during shaving.

Optional: This step should be done the day before the injury to avoid any presence of hair that might contaminate the surgical wound. However, it can also be done during the preparation of the animal just before the laminectomy step.

Table 1. Tables for calculating the volume of drugs

		Volume (μL)									
Analgesic		Number of mice (~25 g)									
Tramadol	Drug dosage	1	2	3	4	5	6	7	8	9	10
	5 mg/Kg	125	250	375	500	625	750	875	1000	1125	1250
Saline	0.9%	200	400	600	800	1000	1200	1400	1600	1800	2000
Total		325	650	975	1300	1625	1950	2275	2600	2925	3250
		Volume (μL)									
Antibiotic		Number of mice (~25 g)									
Enrofloxacin	Drug dosage	1	2	3	4	5	6	7	8	9	10
	5 mg/Kg	125	250	375	500	625	750	875	1000	1125	1250
Saline	0.9%	200	400	600	800	1000	1200	1400	1600	1800	2000
Total		325	650	975	1300	1625	1950	2275	2600	2925	3250

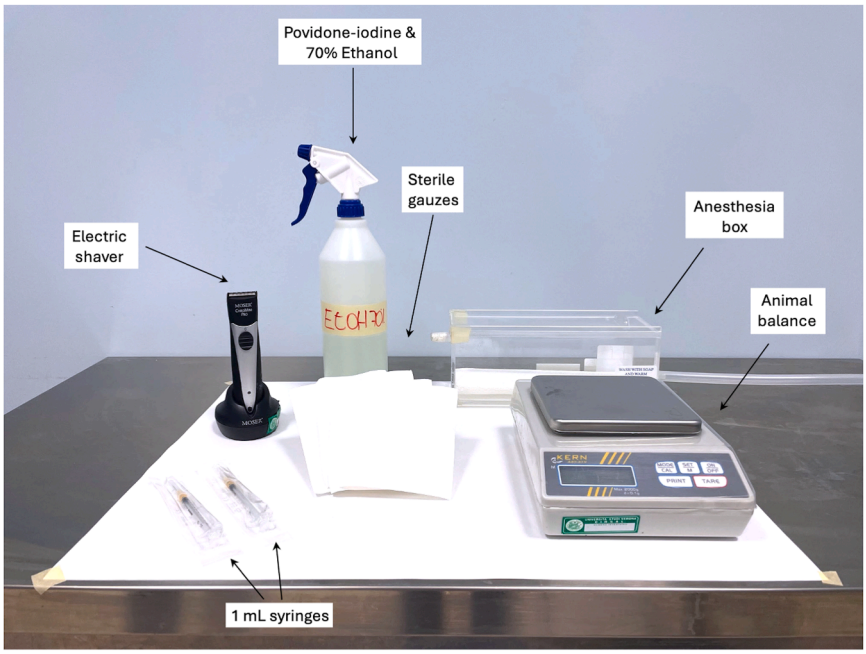

Figure 2. Mouse preparation station
Organization of the bench for the mouse preparation station.

Preparation of the surgical setup

Timing: 45–60 min

2. Disinfect the surgery benches housing the stereo microscope and the NYU-MASCIS II impactor with 70% ethanol (Figures 1A and 1B).

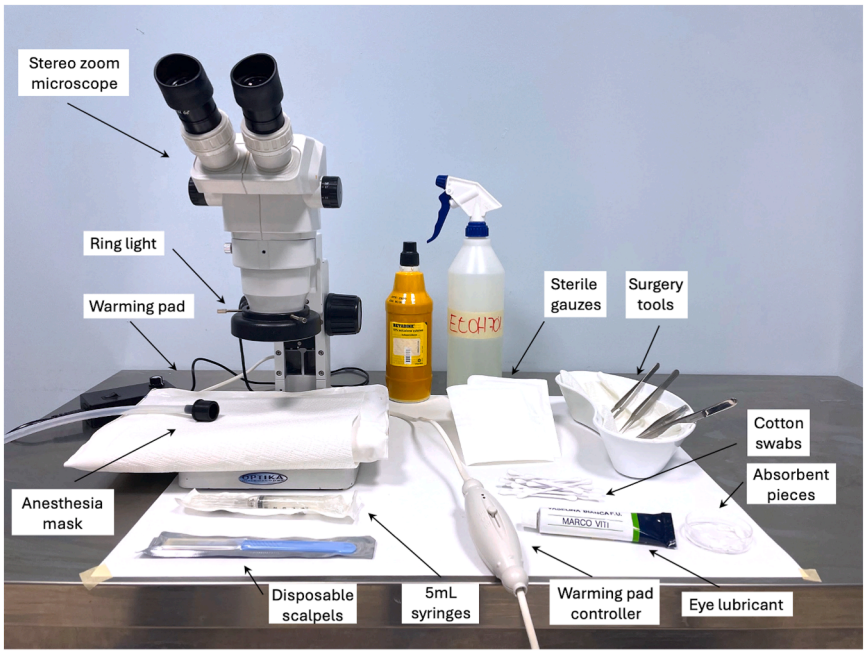

Figure 3. Laminectomy station
Organization of the surgery bench for the laminectomy station.

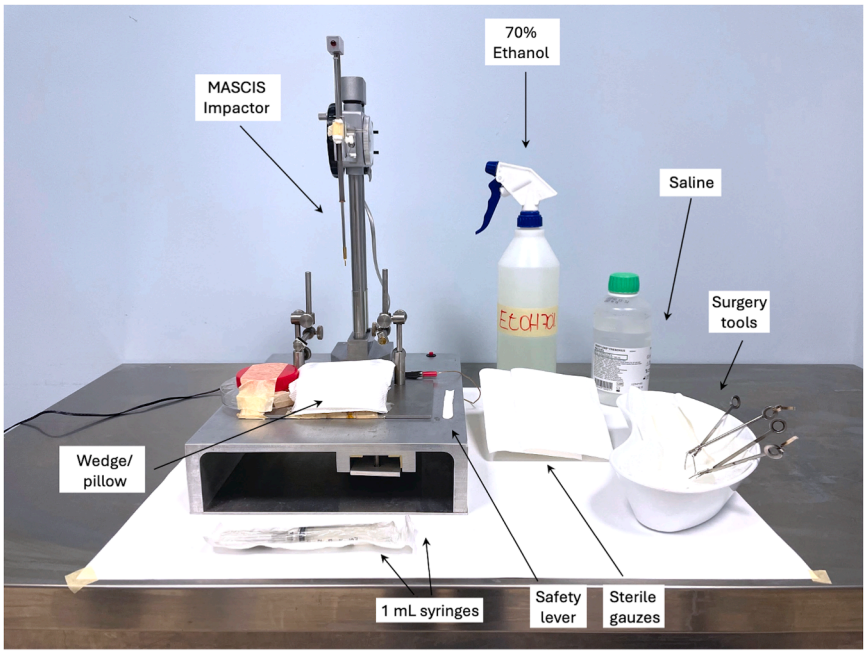

Figure 4. Spinal cord injury station

Organization of the surgery bench for the spinal cord injury station.

3. Laminate the surgery benches with laboratory bench paper and secure them with tape.
4. Arrange the required material for the surgery.

Note: Required material: medical bowls containing enzymatic disinfectant solution and surgical tools, cotton swabs and Petri dish for absorption pieces, ophthalmic lubricant, and sutures, bowl containing povidone-iodine solution; 1 mL syringes for drugs and saline; 5 mL syringe (without needle) containing saline solution; warming pad (refer to Part 1) and Infrared warming lamp; impactor metal stage and spinal column holders (for thoracic surgery) (part of the NYU-MASCIS II impactor system, see key resources table) to secure the mouse's spinal column during the injury phase and create the spinal contusion model.

⚠ CRITICAL: The impactor metal stage consists of a metal plate with two metal arms where fix the spinal column holders. To facilitate the access to the spinal cord, apply a pillow/wedge on the Impactor metal plate which will to lift the upper back of the mouse.

5. Sterilize surgical tools and supplies, including forceps, fine scissors, spring scissors, spinal column holders in the enzymatic disinfectant for at least 20 minutes before the use and put them in the enzymatic disinfectant after each use.

Table 2. Summary of the anesthetic protocol used

Phase	Anesthetic agent	Concentration (%)	Duration	Notes
Induction	Isoflurane	5%	~2–3 min	Administered via induction chamber with 100% oxygen (1.5 L/min flow rate)
Maintenance (initial)	Isoflurane	2.5%	First few minutes	Delivered via nose cone; depth of anesthesia monitored closely
Maintenance (ongoing)	Isoflurane	1–2%	Variable	Titrated based on physiological parameters (e.g., respiratory rate, pedal reflex)
Recovery	—	0%	Until full recovery	Mice maintained under oxygen until spontaneous movement resumed

All procedures were performed on adult C57BL/6 mice.

A 5% concentration of isoflurane was used during induction to ensure rapid onset of anesthesia.

During maintenance, the concentration was reduced progressively, often to as low as 1.5%, based on physiological monitoring to minimize anesthetic exposure.

Note: Dry the surgery tools with absorption paper before each use.

Alternatives: Surgical tools and supply can also be sterilized with the autoclave. In this case, wrap them all in aluminum foil and autoclave them at a temperature of 130°C and 207 kPa (pressure) for 10 minutes. Surgical tools and supply can be autoclaved in advance and stored till their use.

6. Cut absorbent pieces (size of ~25 mm^2) using sterile scissors and transfer them in a sterile Petri dish.
7. Laminate the warming pad with absorption paper to prevent from being soiled and place them one under the microscope.

Note: The warming pad should be easily viewed through the microscope (Figure 1A)

8. Laminate the warming pad with absorption paper at the suture station (Figure 6).
9. Switch on the warming pads (target temperature: ~30°C).
10. Connect the NYU-MASCIS II impactor to the power grid.
11. Fill the vaporizer of the VetEquip rodent anesthesia machine with isofluorane and turn it on.

Setting up the mouse preparation station

Timing: 10 min

12. Prepare the appropriate volume of antibiotic and painkiller to treat mice. Please refer to Table 1 for calculating the volume of drugs.
    a. Enrofloxacin (Baytril, 5 mg/Kg body weight);
    b. Tramadol (Altadol, 5 mg/Kg body weight).
13. Draw the analgesic and the antibiotic into labeled 1 mL syringes fitted with a 25-gauge needle.
14. Gather the required material and lay it on a clean surface (that has been decontaminated with 70% ethanol) for easy access during the mouse preparation (Figure 2).

Note: Required material: electric shaver, 1 mL syringes containing the drugs for the pre-surgical preparation of the mice, wet paper towel/sterile gauzes with 70% ethanol to gently wipe the shaved area on the back of the mouse to remove any loose hair that may have settled on the skin during shaving.

Preparation of the laminectomy station

Timing: 10 min

15. Gather the required material and lay it on a clean surface (that has been decontaminated with 70% ethanol) for easy access during the laminectomy of T11 vertebra (Figure 3).

Note: Required material: cotton swabs and Petri dish for absorbent pieces, ophthalmic lubricant, povidone-iodine and 70% ethanol solutions, disposable scalpel, medical bowls containing enzymatic disinfectant solution and surgery tools, 5 mL syringe (without needle) containing saline solution, cut absorbent pieces (size of ~25 mm^2) in a sterile Petri dish, sterile gauzes.

Preparation of the spinal cord injury station

Timing: 10 min

16. Equip the NYU-MASCIS II impactor with the specific weight for mice (5 grams rod) and gently wipe the Impactor tip with a wet towel paper with 70% ethanol.
17. Gather the required material and lay it on a clean surface (that has been decontaminated with 70% ethanol) for easy access during the spinal injury surgery (Figure 4).

Note: *Required material:* a bowl containing enzymatic disinfectant solution and the spinal column holders (for thoracic surgery) (part of the NYU-MASCIS II impactor system, see key resources table) to secure the mouse's spinal column, impactor metal stage (for thoracic surgery) (part of the NYU-MASCIS II impactor system, see key resources table) to support the spinal column holders (for thoracic surgery) (refer to Part 2), a 5 mL syringe (without needle) with sterile saline solution to be dropped on the spinal cord to avoid the dehydration during the holding phase, a piece of cardboard used to prevent accidental rod release without pressing the start button on the NYU-MASCIS II impactor, sterile gauzes.

Preoperative procedures

Timing: 10 min

18. Switch on the anesthesia machine, set the Isofluorane Vaporizer to 5% for deep anesthesia induction, and the O_2 flow rate to 1.5 mL/min.

Note: A detailed summary of the anesthetic protocol, including concentrations used at each phase, is provided in Table 2.

19. Weigh the mouse (7-week old) and anesthetize it by placing it inside the anesthesia box, which prevents escape (Figure 2) (troubleshooting 1).

⚠ CRITICAL: From the moment the mouse begins anesthesia induction, it must be continuously monitored to prevent respiratory distress, which could result in death.

Note: To obtain a standardized model with results consistent with those presented in this study, we recommend performing the thoracic injury on mice aged between 6 and 8 weeks. Emerging preclinical evidence highlights age as a biological variable that influences the pathophysiology of SCI.

20. After 3–5 minutes, determine if the mouse is anesthetized by pinching one of the hind paws to trigger the pedal reflex response.

Note: If the mouse is fully anesthetized the pedal reflex will be absent.

⚠ CRITICAL: Only when the mouse is unresponsive, proceed to the next step.

21. If not done previously (as suggested), gently wipe the shaved area on the back of the mouse with a wet paper towel soaked in 70% ethanol to remove any loose hair that may have settled on the skin during shaving.
22. Using the labeled 1 mL syringes fitted with a 25-gauge needle, administer the analgesic (tramadol, Altadol) and antibiotic (enrofloxacin, Baytril) subcutaneously (please refer to Table 1 for calculating the volume of drugs).

KEY RESOURCES TABLE

REAGENT or RESOURCE	SOURCE	IDENTIFIER
Antibodies		
Anti-mouse NeuN (1:200)	Millipore	#MAB377
Anti-rabbit NF200 (1:200)	Sigma	#N4142
Anti-goat glial fibrillary acidic protein (GFAP) (1:200)	Abcam	#AB53554
Anti-mouse AlexaFluor 488 (1:1,000)	Thermo Fisher Scientific	#A21202
Anti-rabbit AlexaFluor 488 (1:1000)	Thermo Fisher Scientific	#A21206
Anti-goat AlexaFluor 488 (1:1,000)	Jackson ImmunoResearch Laboratories	#705-545-003
Chemicals, peptides, and recombinant proteins		
Tramadol (50 mg/mL)*	Formevet	Altadol
Enrofloxacin (50 mg/mL)	Bayer	Baytril
Saline (sodium chloride 0.9% w/v)	Fresenius	B230551
Povidone-iodine (10% solution)	MEDA PHARMA spa	023907076
Ophthalmic lubricant	Marco Viti	2909246959
Isoflurane Iso-Vet*	Boehringer Ingelheim Italia S.p.a	103120022
Brilliant blue	Sigma-Aldrich	S3382
Li_2CO_3	Sigma-Aldrich	255823
Ethanol 70%	Generic	Generic
Experimental models: Organisms/strains		
Mus musculus C57BL/6 male/female 7-week-old	Charles River Laboratories/Envigo	
Other		
Weight-drop impactor	NYU MASCIS II impactor system	
Electric shaver	Moser ChroMini Pro	Mod 1591Q
Infrared warming lamp	Mimsal	I-250
Warming pad	Generic	Generic
Paper tape	Generic	Generic
Aluminum foil	Generic	Generic
Sheet protector	Generic	Generic
1 mL syringe with 25-gauge needle	Chemil	S01G25
5 mL syringe	BD Plastipak	308062
Cotton swabs	Generic	Generic
Suture forceps (hemostatic forceps)	B. Braun	BH134R
Scissors	Hebu	HB7470
#4 forceps	FST	11241-30
Extra-fine forceps (#5SF)	FST	11223-20
Toothed forceps	Ulrich	U14-933-20
Spring scissors (extra fine)	Hebu	HB7380
Absorption pieces	Generic	Generic
Suture 6-0	VetSuture Silk	SILK15CN
Stereo zoom microscope	Optika Microscope	SZ6745
Ring light source (led lamp)	Cicony	15917685217440
Disposable scalpel	Chemil	SCA22w
VetEquip rodent anesthesia machine	VetEquip	901806
Sterile gauze	Rays	C29X3N1SZ6II

MATERIALS AND EQUIPMENT

Critical considerations

- Since some drugs may be classified as controlled substances based on local laws and regulations, the appropriate indications regarding storage, use, and disposal must be followed (marked with an asterisk in the related key resources table).

- All steps handling drug handling must be conducted wearing gloves and in compliance with relevant safety regulations.
- All procedures involving animals must be conducted in accordance with institutional guidelines for the care and use of animals in research.
- While C57BL/6 mice have been used in this protocol, it could be extended to CD1 mice without requiring optimization.

Possible alternatives

- A standard surgical or dissection microscope with 5–10× magnification is suitable for the laminectomy step. When performing the laminectomy at thoracic T11 vertebrae level, tilt the microscope to provide sufficient clearance and visibility, as it is crucial to avoid damaging the spinal cord during this procedure.
- Although this protocol uses the NYU-MASCIS II impactor, a severe contusive-compressive SCI could be achieved using the Infinity Horizon (IH) impactor with parameters of 60 or 70 KDyne force and 11 seconds dwell time. This produces comparably severe contusive-compressive injuries (BMS score at 1 dpi: NYU-MASCIS II impactor: 0.06 $\pm$ 0.17, n=39; IH impactor: 0.0 $\pm$ 0.0, n=6; and at 7 dpi: NYU-MASCIS II impactor: 0.46 $\pm$ 0.57, n=39; IH impactor: 0.083 $\pm$ 0.20, n=6).
- This injury model has been validated in both male and female C57BL/6 and CD1 mice, showing comparable BMS outcomes across sexes and strains, supporting its reproducibility.
- If an infrared warming pad is unavailable, alternatives such as hand warmers or gel-based heating pads may be used. However, it is essential to regularly monitor the temperature to ensure it is not too hot or too cold.

STEP-BY-STEP METHOD DETAILS

This section provides detailed instruction for: (a) exposing the spinal cord parenchyma at the T11 vertebrae level, (b) performing the severe contusive-compressive spinal cord injury, and (c) postoperative care following surgery.

Operative procedure for thoracic spinal segment exposure (laminectomy)

Timing: 15 min

Here we describe how to perform surgery to expose the T11 thoracic spinal segment for severe contusive-compressive spinal cord injury. Upon completion of the following steps, the T11 segment will be fully accessible for injury (Figure 5).

1. Transfer the anesthetized mouse to the surgical area and place it ventral side down on the heating pad.
2. Prepare the mouse for surgery (troubleshooting 7).

⚠ CRITICAL: Ensure that the anesthesia mask is correctly positioned so that the mouse can be easily viewed through the microscope. Secure the mask with tape on the absorption paper covering the surgery bench.

3. Sterilize the surgical site by swabbing the skin with povidone-iodine solution (Figure 5A).
4. Apply ophthalmic lubricant to both eyes to prevent drying during surgery (Figure 5A).
5. Using a scalpel, make a 2 cm midline skin incision, starting at the base of the head and extending down the midline of the back (Figures 5B and 5C).
6. Identify the T11 vertebra using anatomical landmarks (Figures 5D and 5E).
   a. Locate the intervertebral space between L3 (identified as the last caudal prominent spinous processes) and L4 (identified as subsequent shorter spinous processes) vertebra,[18]
   b. From L4, count seven vertebral processes rostrally to locate the T11 vertebra.

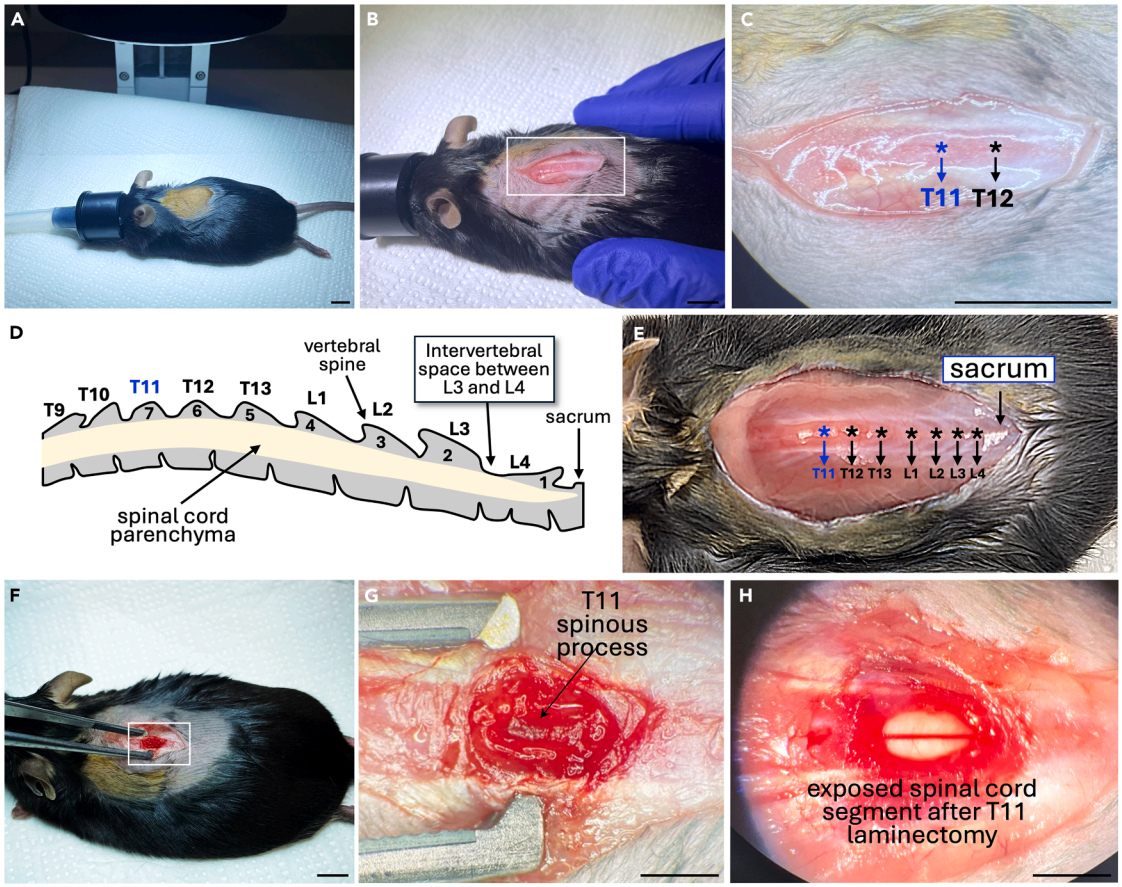

Figure 5. Representative images of a mouse at different stages of thoracic laminectomy

(A) Anesthetized mouse at the surgical area under the stereo microscope. The underside of the mouse is exposed to the heating pad. The surgical site is sterilized with Povidone-iodine solution and the ophthalmic lubricant was applied. Scale bar: 1 cm.

(B) Image showing the skin incision made on the back of the mouse, exposing the underlying tissue.Scale bar: 1 cm.

(C) Magnification of the white box in (B) highlighting the underlying musculature at T11 and T12 vertebrae level.Scale bar: 1 cm.

(D) Schematic illustration of the thoracic and lumbar vertebrae to facilitate identification of the T11 thoracic vertebra (blue). We highlight as anatomical landmark the intervertebral space between L3 (identified as the last caudal prominent spinous process) and L4 (identified as subsequent shorter spinous process).

(E) Exposed dorsal region of the mouse showing anatomical landmarks for identifying the T11 thoracic vertebra (blue). Each vertebra was marked with an asterisk to facilitate accurate segmental identification.

(F) The paraspinal muscles were dissected away and the underlying T11 spinous process and lamina were revealed. Scale bar: 1 cm.

(G) Magnification of the white box in (F) showing the cleaned T11 vertebra. The black arrow indicates the T11 spinous process.Scale bar: 1 cm.

(H) Image showing the exposed spinal cord segment under the T11 vertebra after performing a laminectomy. Scale bar: 1 cm.

7. Using micro scissors, cut the rostral paraspinal muscles attached to the T11 vertebra.
   a. Carefully slide the micro scissors underneath the rostral musculature.
   b. Cut along the midline to detach it from the underlying thoracic vertebrae (troubleshooting 2).
8. Using spring scissors and the #4 forceps, dissect the paraspinal muscles away from the T11 spinous process and lamina (Figures 5F and 5G).

⚠ CRITICAL: Ensure complete removal of residual tissue to clearly expose the vertebrae.

9. Identify the T11-T12 vertebral junction.
10. Remove the tissue connecting the T11 and T12 vertebra to expose the underlying spinal segment (troubleshooting 2).

Figure 6. Representative images of a mouse at different stages of severe contusive-compressive SCI

(A) Anesthetized mouse at the surgical area stabilized on the Impactor metal stage. Dotted line highlights the optimal positioning of the spinal column (parallel to the surface of the Impactor metal plate). Scale bar: 1 cm.

(B) Mechanical clamp of the NYU-MASCIS II impactor clamping one of the cut flaps of skin of the back of mouse. Scale bar: 1 cm.

(C) Safety cardboard between the Impactor tip and the exposed spinal cord parenchyma. Scale bar: 1 cm.

(D and E) Representative images and relative magnifications of the injured spinal cord segment under the T11 vertebra immediately after the spinal injury (D) and after 1 minute (E) highlighting the hematoma developed following SCI. Scale bars: 1 cm.

Note: The specific spinal segment to be exposed depend on the research interest. For thoracic SCI, levels T9–T12 are the most commonly used due to their consistency and ease of standardization.

11. Stabilize the spinal column at T12 vertebrae with toothed forceps while removing the spinous process and lamina of T11 (laminectomy) to expose the spinal cord parenchyma (troubleshooting 2).

⚠ CRITICAL: Stabilize the spine gently but firmly, excess pressure can damage the integrity of T12 vertebrae and increase bleeding.

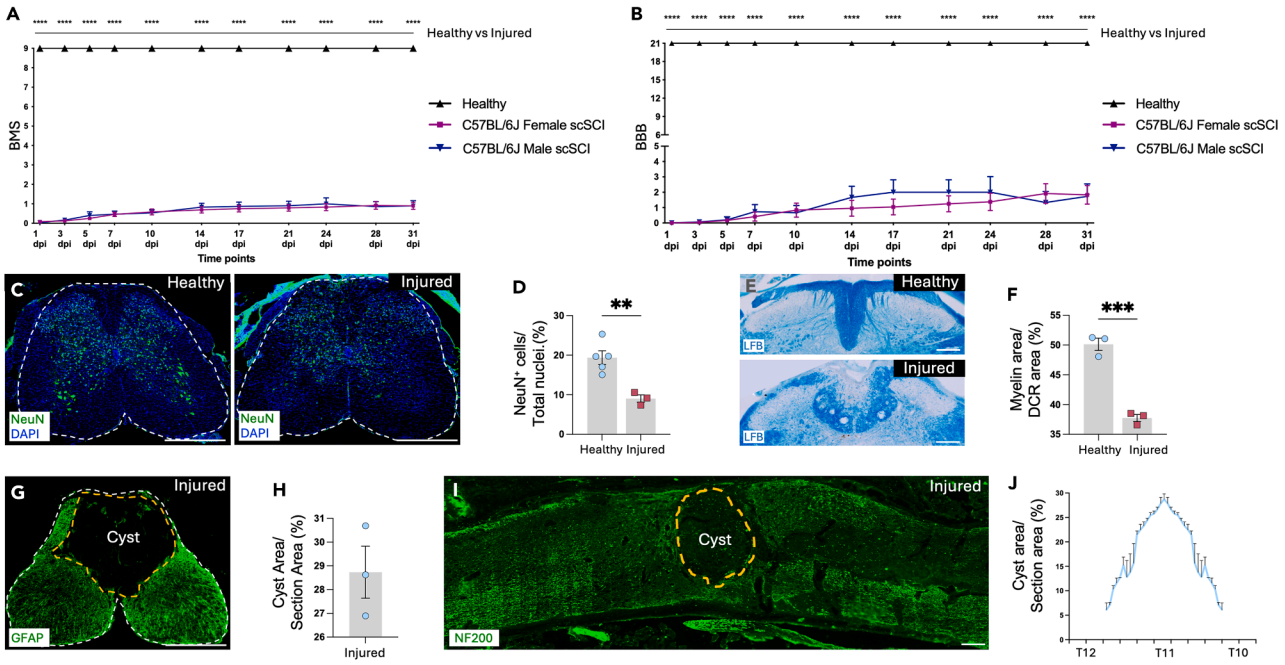

Figure 7. Expected locomotor and neural tissue outcomes following severe contusive-compressive SCI (31 dpi)

(A) Locomotor evaluation (BMS) at 31 dpi of healthy, female, and male C57BL/6 severe contusive-compressive SCI (scSCI) mice. scSCI mice showed severe loss of locomotor functionality compared to healthy mice. Female (n=24) and male (n=14) scSCI mice exhibited comparable severe impairments.

(B) Locomotor evaluation (BBB) at 31 dpi of healthy, female, and male C57BL/6 scSCI mice. scSCI mice showed severe loss of locomotor functionality compared to healthy mice. Female (n=24) and male (n=14) scSCI mice exhibited comparable severe impairments.

(C) Transverse sections from healthy and scSCI spinal cords showing the neuronal content (NeuN marker, green). Injured mice showed reduced neuronal content. Scale bar: 500 μm.

(D) Graph showing the percentage of NeuN+ cells in healthy and scSCI mice.

(E) Magnification of the dorsal column region from transverse sections of healthy and scSCI spinal cords showing the myelin content (Luxol Fast Blue staining, LFB). scSCI mice showed reduced myelin content. Scale bar: 200 μm.

(F) Graph showing the percentage of myelin content in healthy and scSCI mice.

(G) Transverse section from a scSCI spinal cord showing the formation of a large cyst (GFAP marker, green). The dotted white lines delineate the section area. The dotted yellow line delineates the cyst area. Scale bar: 500 μm.

(H) Graph showing the cyst area (%) in scSCI mice.

(I) Longitudinal section from a scSCI spinal cord showing the NF200 content (NF200 marker, green). Scale bar: 200 μm.

(J) Graph showing the percentage of cystic area in successive transverse spinal cord sections in scSCI C57BL/6 mice covering the region from T12 to T10. The lesion is localized exclusively at the T11 vertebra level, with no spread to adjacent segments.

12. Using the #S5 forceps, enter the intrathecal space between T11-T12 vertebrae and remove the T11 lamina piece by piece (Figure 5H) (troubleshooting 2 and 5).

Note: Remove the lamina in small fragments to minimize bleeding. Avoid attempting to remove large portions at once.

⚠ CRITICAL: Ensure that the edges of the vertebral canal are fully cleared, as any residual bone could interfere with the following spinal cord injury process. A clean injury site guarantees maximum energy transfer from the weight drop to the spinal cord.

13. Apply a drop of sterile saline onto the exposed spinal segment under T11 vertebra to prevent dehydration.

Operative procedure for thoracic contusive-compressive injury surgery

Timing: 12 min

Table 3. Pain score assessment table

Clinical manifestation	Score
Normal fur, normal mucosa, normal physical activity, normal food and water intake	0
Ruffled fur (piloerection, lesions, dehydration)	1
Abrasions and/or wounds (small size, bite marks, scratches)	2
Ruffled fur, < physical activity (grooming, exploration…)	2
Abnormal feces (very dry, very wet)	2
Ruffled fur, ↓ physical activity (lethargy),[a] weight loss < 10%	3
Ruffled fur, lethargy, [a]weight loss < 10%, respiratory difficulty (dyspnea, tachypnea)	4
Abrasions and/or wounds (extensive, presence of mutilations)	4
Ruffled fur, lethargy, [a]weight loss between 10 and 20%, dyspnea/tachypnea, lordosis/kyphosis	5
Abnormal breathing (gasping)	5
Ruffled fur, lethargy, dyspnea/tachypnea, lordosis/kyphosis, [a]weight loss > 20%	6

[a]Note: Weight is relative to expected values for age and sex.

14. Quickly transfer the mouse to the spinal cord injury station.
15. Place the mouse on the metal stage of the Impactor device (troubleshooting 7).

Note: Insert a wedge beneath the mouse to facilitate access to the spinal cord.

16. Stabilize the mouse on the metal plate using the spinal column holders, with the forelimbs and hindlimb fully extended (Figure 6A).

Note: The spinal column holders should be applied to the lateral spinous processes immediately rostral and caudal to the laminectomy site (troubleshooting 3).

⚠ CRITICAL: After stabilization, ensure that the spinal cord is perfectly parallel to the surface of the impactor metal plate. If not, adjust the position of the spinal column holders accordingly.

17. Attach one of the skin flaps to the mechanical clamp of the NYU-MASCIS II impactor (Figure 6B).
18. Carefully slide the metal stage under the Impactor tip.
19. Lower the tip to a few millimeters above the spinal cord to ensure it is precisely centered over the T11 segment.

⚠ CRITICAL: Verify that the impactor tip is accurately aligned with the laminectomy window. If not, reposition the mouse adjusting the position of the Impactor metal stage until optimal alignment is achieved (troubleshooting 8).

Table 4. Human endpoint criteria

Human endpoint criteria
Persistent lordosis/kyphosis with clinical signs of suffering (≥3)
Inability to access food and/or water
Seizures
Self-mutilation
Weight loss >20% compared to expected
Significant behavioral changes (e.g., depression, ataxia, lethargy)
Presence of injuries (e.g., pressure ulcers, self-inflicted wounds, bleeding)
Marked decrease in food or water intake
Penile prolapse
Tremors or abnormal pain-related behaviors (e.g., abdominal contraction, rolling on the side)

20. Slowly lower the Impactor tip until it gently touches the aligned spinal cord segment, as confirmed by the activation signal of the NYU-MASCIS II device.

Note: This step is essential to accurately set the drop height. When the rod tip makes contact with the spinal cord, the device emits an auditory signal confirming both contact and system functionality (troubleshooting 4).

21. Press the designated button to zero the height calibration system.
22. Set the injury parameters based on the desired injury severity.

Note: For a severe contusive-compressive SCI in C57BL/6 mice, use a 5 g rod dropped from a 6.25 mm and 11 seconds compression, corresponding to an impact velocity of 0.35 m/s, force of 0.31 mJ and an impact force of 61.3 KDyne (E = mgh = 0.005·9.81·0.00625=0.00030656J ≈0.31mJ; F = 0.00030656/0.0005 = 0.613N = 61.3 KDyne; displacement value of 0.5 mm[13,14]). The NYU-MASCIS II impactor does not provide real-time force applied or depth feedback. Injury reproducibility is ensured by strict control of rod weight and drop height, in accordance with validated. On the base of the age and injury severities parameters may need to be adjusted.

23. Insert the safety cardboard between the Impactor tip and the exposed spinal cord (Figure 6C) and keep it in place until just before the injury induction.

⚠ CRITICAL: To prevent uncontrolled Impactor tip release (which can result in an uncontrolled lesion with undefined dwell time), retain the cardboard (referred to as safety cardboard) barrier until the moment the start button is pressed.

24. Remove the safety lever that locks the weight release mechanism.
25. Remove the safety cardboard.
26. Press the starting button to deliver the injury.
27. Allow the weight to compress the spinal cord for 11 seconds.

Note: Use a timer to ensure precise dwell time control.

28. Gently raise the Impactor tip and release the spinal column holders.
29. Immediately transfer the mouse to the suture station and visually confirm the injury (Figures 6D and 6E).

Note: A hematoma should begin forming immediately post-injury (Figure 6D) and enlarge over time (Figure 6E), consistent with severe mechanical damage.

30. Suture the skin using 4-0 silk to close the wound.

Alternatives: Skin closure may also be performed using autoclips and the appropriate applicator.

31. Administer 1 mL of sterile saline solution subcutaneously for hydration using a 1 mL syringe.

Post-operative care

Timing: 10 min

32. Return the mouse to its home cage, placing it under a worming lamp, with easy access to food and water.

Note: Adjust the distance between the cage and the lamp to prevent overheating. The optimal ambient temperature should be maintained between 25°C–27°C.

33. Continuously monitor the mouse and provide post-operative care.

Note: Due to impaired hindlimb function post-SCI, place food pellet on the cage floor throughout the experiment to ensure access.

⚠ CRITICAL: The mouse should awaken within 3–5 minutes and begin to ambulate within 10 minutes of removal from the anesthesia mask (troubleshooting 9). Mice with severe contusive-compressive SCI mice may display pronounced hindlimb motor deficits immediately upon awakening.

34. Starting from the day after the surgery, administer analgesic (Tramadol, Altadol) subcutaneously for 2 days post-injury and antibiotic (enrofloxacin, Baytril) for 5 days (please refer to Table 1 for calculating the volume of drugs), using a 1 mL syringe with a 25-gauge needle starting from the day after the injury surgery.

Note: While handling the mice for drug administration, avoid manipulating the wound or sutures.

35. Manually express the bladder.

Note: Manually express the bladder twice daily during the first week post-injury, then once daily until the end of the experiment, using the Credè maneuver.[19] This involves applying gentle pressure to the lower abdomen with the thumb and forefingers. A standardized technique is provided in Methods video S1 (troubleshooting 10).

⚠ CRITICAL: On the day of the injury, express the bladder only once.

36. Monitor all animals daily using a clinical scoring system to assess pain and distress (troubleshooting 6).

⚠ CRITICAL: Assess pain and distress using a standardized clinical scoring system (please refer to Table 3), and predefined humane endpoint criteria (please refer to Table 4) to ensure ethical compliance. Animals reaching a clinical score ≥6 or meeting one or more endpoint criteria, along with the ethical authorization of the institution, have to be euthanized to prevent further distress.

37. At the end of the experiment (31 days post-injury), sacrifice the mice by perfusion and collect the spinal cords for histological analysis. (Figure 7).

Note: The duration of the experiment can be modified depending on the research objectives.

EXPECTED OUTCOMES

The severe contusive-compressive SCI model proposed, induces a profound impairment to the neural tissue resulting in a permanent and complete loss of motor functions.[5] Some advantages of the technique we present over other methods of spinal injury are that: i) while commonly used rodent models spontaneously and rapidly recover after SCI, this contusive-compressive model leads to complete paralysis of the hind limbs without spontaneous functional recovery; ii) injured mice exhibited neurobiological alterations in the spinal cord, faithfully replicating the injury response observed in humans with complete SCI; iii) injured mice exhibited the main secondary reactions

occurring during the subacute phase following injury such as cell loss, inflammatory cell infiltration, tissue ischemia, and the disruption of the extracellular architecture associated with the formation of a large cyst; iv) the model has been successfully applied in both female and male C57BL/6 and CD1 mice without requiring optimization, yielding comparable injury severity and functional outcomes across sexes; however, slight sex-related differences in recovery may occur due to inherent biological variability, including hormonal and anatomical factors that should be considered when interpreting results; v) the use of inhaled anesthesia rather than injectable anesthesia circumvents the need of further injections to the animals. To enhance reproducibility, animals with a BMS score greater than 0.5 at 1 dpi are excluded from the experimental groups, as this criterion helps reduce variability by selecting only animals with comparable injury severity. In our experiments, the exclusion rate was approximately 9% of the injured animals.

31 days after the contusive-compressive injury, a reduction of neuronal content should be seen in the rostro-caudal region of the cord spanning the spinal segment which underwent the lesion. To validate the efficacy of the spinal injury we performed locomotor function analysis using the BMS and BBB-adapted scoring scale[13,20] (Figures 7A and 7B), *in vivo* electromyography (EMG) analysis and histological analysis. These included evaluation of neuronal (Neun marker-positive cells normalized for the total nuclei of the slice, Figures 7C and 7D) and myelin content (Luxol Fast Blue staining, LFB positive-pixel over the total pixel of the central column region, Figure E, F), and the formation of a large cyst which almost occupied the whole transversal spinal section (GFAP staining)[5] (Figures 7G and 7H) and is localized exclusively at the T11 vertebra level (Figures 7I and 7J). To this aim, we collected the spinal cords (following cardiac perfusion with 10 mL of PBS solution followed by 10 mL of 4% PFA 4% sucrose in PBS solution), after 24 hours of incubation in 4% PFA 4% sucrose in PBS solution at 4°C, we cryo-preserved the spinal cords leaving them in 30% sucrose at 4°C till the time of their processing. To analyze the cords, we embedded them in cryo-embedding compound (OCT) and cut transverse or longitudinal sections (25 μm thickness).

Typically, following severe contusive-compressive SCI mice underwent grave disability which can already be observed early as awakening from anesthesia and could be further verified with the functional and histological analysis. Specifically, at 31 dpi, female C57BL/6 mice (n = 24, from three independent experiments) showed an average BMS score of 0.90 ± 0.18 SEM (adapted-BBB: 1.83 ± 0.61), these results were comparable to what observed for male mice (n = 14, from three independent experiments) showing an average BMS score of 0.89 ± 0.27 SEM (adapted-BBB: 1.73 ± 0.81) (female C57BL/6 SCI mice vs male C57BL/6 SCI mice at 31 dpi both BMS and adapted-BBB: p=0.9999, Figures 7A and 7B). We have also collected BMS data from female and male CD1 mice (n = 9, from two independent experiments) up to 7 dpi, showing a mean BMS score of 0.33 ± 0.14 SEM, indicative of consistent severe locomotor deficits in this strain (C57BL/6 SCI mice vs CD1 SCI mice at 7 dpi: p= 0.9732). Muscle paralysis was assessed by averaging the root mean square (RMS) values of the 10 largest electromyography (EMG) signals. Lumping together *Tibialis Anterior* (TA) and *Lateral gastrocnemius* (LG) muscles, RMS of injured animals was 5.7 ± 0.71 μV (n=20), which is significantly smaller than the value measured in control muscles (10.5 ± 1.14 μV n=15). After immuno- and/or histological staining, the neuron and myelin content in the spinal parenchyma of injured mice should be reduced compared to the ones of controls (Figures 7C–7F). At the site of the injury a large cyst surrounded by glial/fibrotic scar is formed[5,21] (Figures 7G and 7H). The lesion is localized exclusively at the T11 level, with no spread to adjacent segments (Figures 7I and 7J).

QUANTIFICATION AND STATISTICAL ANALYSIS

Locomotor evaluation. The locomotor function of both control and injured mice was evaluated using the Basso Mouse Scale.[13] All assessments were conducted in a blinded manner by at least two observers. Locomotor performance was monitored for 4 minutes in an open field at 1, 3, 5, 7, 10, 14, 17, 21, 24, 28, and 31 dpi (day post injury). To improve the evaluation of locomotor function in animals with low BMS, we employed a refined locomotor assessment protocol based on the methodology

described by.[20] In particular, we utilized a modified version of the Basso, Beattie, and Bresnahan (BBB) scoring system to enhance sensitivity in detecting subtle yet functionally relevant differences between experimental groups. This adapted scoring approach includes additional qualitative and quantitative parameters—such as paw placement accuracy, consistency of stepping patterns, and the extent of forelimb–hindlimb coordination—allowing for a more detailed evaluation of locomotor function, especially in animals demonstrating partial recovery. To ensure injury severity consistency, only animals with a BMS or BBB score ≤ 0.5 at 1 dpi were included in the study. *LFB staining.* The myelin content in the spinal cord sections was quantified *via* LFB staining (Sigma-Aldrich) as described.[21] *Immunofluorescence staining.* Cryosections were immunostained as described[21] and relative images were acquired using a 20× objective on a Nikon Ti Eclipse fluorescent microscope. In vivo *electromyographic (EMG) recording: In vivo* electromyographic recordings of spontaneous voluntary muscle activity were performed in the Tibialis Anterior (TA) and Lateral Gastrocnemius (LG) muscles bilaterally. Two thin stainless-steel wires (125 μm diameter) with exposed tips were inserted longitudinally into each muscle of anesthetized animals (please refer to Table 2) and connected to an amplifier (CyberAmp 320, Axon Instruments, USA) for differential recording, in order to maximize EMG selectivity. A shortened 20G stainless steel needle was inserted subcutaneously in the animal's back to serve as the reference (ground) electrode. EMG signal was amplified 5000x, 100-1200 Hz band pass filtered, further improved with hum pick-up suppression (Hum-Bug, Quest scientific, USA), digitized at 10 KHz and acquired with Signal software (version 6.0.2, Cambridge Electronic Design, UK). Recordings started 10 minutes after the animals had fully recovered from anesthesia and lasted for 3 minutes per muscle. During this time, animals were gently stimulated every 10–15 seconds to encourage movement. To reduce movement artifacts, the animal was contained in ventral decubitus with tapes across the body, the limbs and the tail. At the end of recording, the animal was re-anesthetized in order to cut either the sciatic nerve bilaterally or the spinal cord at T10 (i.e. cranially to spinal cord injury level). A second session of recording was then initiated 10 min after full recovery from anesthesia, and lasted 1 min for each muscle. At the end of the experiment, the animal was euthanized with excess of anesthesia. EMG signal was processed off-line with Signal 6.0.2 and Spike2 5.0.9 software (Electronic Design, Cambridge, UK). Amount of muscle paralysis was determined with: i) quantification of the power of the electrical signal during contractions by measuring its Root Mean Square (RMS) value and ii) quantification of the duration of the electrical signal during contractions. To measure RMS, every EMG trace was divided into 40 ms-long sections and RMS calculated in each section with a time constant of 10 ms. RMS values bigger than a cutoff level were considered as related to voluntary muscle activity. In each muscle the cutoff level was determined as the average RMS (+1.9 standard deviations) measured after sciatic nerve or spinal cord section. Finally, we extracted RMS values corresponding to the periods of strongest muscular activity, by averaging the 10 largest RMSs among all the measured values. To quantify the total duration of muscle activity, we multiplied the total number of above-cutoff trace sections by 0.04 (i.e. the duration of each section). Lumping together TA and LG muscles, RMS of injured animals was 5.7 ± 0.71 microV (n=20), which is significantly smaller to the value measured in control muscles (10.5 ± 1.14 microV n=15). Quantification and statistical analysis. Quantitative analysis was performed using ImageJ software (National Institutes of Health, USA). For each biological replicate, a minimum of 2 technical replicates were analyzed, and the minimum number of biological replicates was 3 animals per group. The following quantification procedures were applied: i) Neuronal cells: The content of $Neun^+$ cells was evaluated in silico in at least 8 transverse spinal cord sections per biological replicate. Results were normalized according to the total number of nuclei in the spinal cord slice; ii) Myelin content (Luxol Fast Blue, LFB): LFB staining was quantified in at least 14 spinal cord per biological replicate, using manual pixel thresholding to identify LFB positive-pixels. Results were normalized according to the dorsal columns region of the spinal cord slice; iii) Cyst area: Cyst area was manually estimated based on the GFAP staining on serial transverse histological images. Results were normalized to the total cross-sectional area of the spinal cord in each slice. All analysis were conducted on serial transverse sections spanning approximately +0.35 cm rostral to −0.35 cm caudal relative to the lesion epicenter. We will integrate these details into the revised manuscript to strengthen the methodological rigor and ensure full

reproducibility of the study. GraphPad Prism software (version 7.0) was used to perform Student t-test and two-way ANOVA with repeated measures. Data are presented as mean ± SEM, and statistical significance was set at $p < 0.05$.

LIMITATIONS

A limitation of this protocol could be its application for cervical injury due to the difficulty in positioning the spinal column holders. Another limitation of this protocol is that real-time information about the applied force, velocity and cord compression was not included.

TROUBLESHOOTING

Problem 1

The mouse suffers from respiratory distress during the surgical procedures (Step 19).

Potential solution

It is likely the percentage of anesthetic is too high. In this case, remove gently the mouse from the anesthetic mask until it returns breathing normally and reduce the percentage of isoflurane. Usually, anesthesia was induced with isoflurane at 2.5% in oxygen and subsequently maintained at 1–2% throughout the procedure, which has been established as the optimal concentration range to ensure adequate anesthesia while minimizing physiological stress. A detailed summary of the anesthetic protocol, including concentrations used at each phase, is provided in Table 2.

Problem 2

Excessive hemorrhaging during thoracic surgery (Step 7, 10, 11, 12).

Potential solution

Bleeding is common in thoracic surgeries. If the bleeding avoids the cleaning procedure, periodically soak the excess of blood using cotton swabs or absorption pieces to obtain a clear view of the spinal segment. To minimize hemorrhaging, take care to preserve the integrity of any blood vessels running along the midline of the spinal cord.

Problem 3

One or both of the spinal column holder do not hold stably the spinal column (Step 16).

Potential solution

Carefully release the spinal column holder/s and adjust its/their position. If it does not work, with the spring scissors make very small cuts laterally along the spinal column at both sides of the spinal column (rostrally or/and caudally). This procedure will increase the grip and thus the stability of the spinal column holder/s. Then apply again the spinal column holder/s taking care to locate them at the level of the small cuts.

Problem 4

When setting the parameter for the injury procedure, the NYU-MASCIS II impactor does not produce any sound signal (Step 20).

Potential solution

It is likely the spinal cord parenchyma is dried. In this case apply a small droplet of saline on the Impactor tip and on the exposed spinal cord. Then, adsorb the excess solution with adsorbent pieces.

Problem 5

The spinal cord surface is not clearly visible during the laminectomy (Step 12).

Potential solution

This may occur due to insufficient bone removal or bleeding. Ensure that the lamina is fully removed using fine rongeurs or micro-scissors. Irrigate the area gently with sterile saline to remove blood or debris. Ensure adequate lighting and adjust the microscope angle to improve visibility. Avoid damaging the dura or spinal cord while cleaning.

Problem 6

Post-surgical infection or wound dehiscence (Step 36).

Potential solution

Infections may result from insufficient aseptic technique or improper closure. Ensure the surgical field is properly disinfected and that sterile tools and gloves are used. Administer post-operative antibiotics as per institutional guidelines if signs of infection appear. Carefully close the skin layer to minimize tension. Monitor daily and re-suture if needed.

Problem 7

Animal shows spontaneous movement during surgery (Step 2, 15).

Potential solution

This indicates inadequate anesthesia depth. Confirm the isoflurane vaporizer is functioning properly. Adjust the anesthesia level temporarily back to 2–2.5% until the mouse is fully sedated, then return to maintenance levels (1–1.5%). Always verify the absence of reflexes before proceeding.

Problem 8

The injury severity is inconsistent across animals (Step 19).

Potential solution

Ensure the spinal cord is centered and immobilized before delivering the injury. Misalignment may result in partial or asymmetric damage. Always confirm the post-injury BMS score at 1 dpi and exclude animals with a score >0.5 to standardize injury severity.

Problem 9

Animal fails to recover from anesthesia post-surgery (Step 33).

Potential solution

Prolonged anesthesia or hypothermia can delay recovery. Ensure the animal is placed on a heated pad post-surgery and monitor breathing and reflexes. Reduce surgical time when possible. If recovery is delayed beyond 10–15 min, gently stimulate the animal and confirm that the airway is clear and unobstructed.

Problem 10

Urine retention in SCI mice (Step 35).

Potential solution

Spinal cord injury often leads to bladder dysfunction. Manual bladder expression should be performed twice daily during the first week post-injury, then once daily until the end of the experiment. Monitor for signs of discomfort, abdominal distension, or wet bedding. If urine is not easily released, consult veterinary staff for supportive treatment.

RESOURCE AVAILABILITY

Lead contact

Further information and requests for resources and reagents should be directed to and will be fulfilled by the lead contact, Ilaria Decimo (ilaria.decimo@univr.it).

Technical contact

Technical questions on executing this protocol should be directed to and will be answered by the technical contact, Sissi Dolci (sissi.dolci@univr.it).

Materials availability

This study did not generate new unique reagents.

Data and code availability

The published article includes all datasets generated or analyzed during this study.

ACKNOWLEDGMENTS

This work was supported by the National Recovery and Resilience Plan (PNRR), Mission 4 Component 2 Investment 1.3 - Call for tender no. 341 of 15/03/2022 of Italian Ministry of University and Research funded by the European Union – NextGenerationEU award number: project code PE0000006, concession decree no. 1553 of 11/10/2022 adopted by the Italian Ministry of University and Research, CUP D93C22000930002, "A multiscale integrated approach to the study of the nervous system in health and disease" (MNESYS). European Union project FETPROACT-2018-2020 HERMES (grant number 824164) is acknowledged for the support on research provided to I.D., G.C., G.P., and J.H. We thank the Italian patient associations "GALM" and "La Colonna" for financial support. We thank "Centro Interdipartimentale di Servizio alla Ricerca Sperimentale-CIRSAL" of the University of Verona and S.R. for technical support.

AUTHOR CONTRIBUTIONS

S.D. and I.D. designed the study. S.D. and M.D.C. performed experiments and imaging and analyzed and interpreted data. G.B. performed EMG recordings and analysis. S.D. wrote the paper. All authors discussed the results and provided comments on the manuscript. I.D. and F.B. supervised the study. I.D. acquired the funds.

DECLARATION OF INTERESTS

The authors declare no competing interests.

SUPPLEMENTAL INFORMATION

Supplemental information can be found online at https://doi.org/10.1016/j.xpro.2025.104029.

REFERENCES

1. y Cajal, S.R. (1991). Cajal's degeneration and regeneration of the nervous system (History of Neuroscience).

2. Marino, R.J., Leff, M., Cardenas, D.D., Donovan, J., Chen, D., Kirshblum, S., and Leiby, B.E. (2020). Trends in Rates of ASIA Impairment Scale Conversion in Traumatic Complete Spinal Cord Injury. Neurotrauma Rep. *1*, 192–200. https://doi.org/10.1089/neur.2020.0038.

3. Kirshblum, S.C., Waring, W., Biering-Sorensen, F., Burns, S.P., Johansen, M., Schmidt-Read, M., Donovan, W., Graves, D., Jha, A., Jones, L., et al. (2011). Reference for the 2011 revision of the International Standards for Neurological Classification of Spinal Cord Injury. J. Spinal Cord Med. *34*, 547–554. https://doi.org/10.1179/107902611X13186000420242.

4. McDonald, J.W., and Sadowsky, C. (2002). Spinal-cord injury. Lancet *359*, 417–425. https://doi.org/10.1016/s0140-6736(02)07603-1.

5. Dolci, S., Mannino, L., Bottani, E., Campanelli, A., Di Chio, M., Zorzin, S., D'Arrigo, G., Amenta, A., Segala, A., Paglia, G., et al. (2022). Therapeutic induction of energy metabolism reduces neural tissue damage and increases microglia activation in severe spinal cord injury. Pharmacol. Res. *178*, 106149. https://doi.org/10.1016/j.phrs.2022.106149.

6. Ahuja, C.S., Wilson, J.R., Nori, S., Kotter, M.R.N., Druschel, C., Curt, A., and Fehlings, M.G. (2017). Traumatic spinal cord injury. Nat. Rev. Dis. Primers *3*, 17018. https://doi.org/10.1038/nrdp.2017.18.

7. Mautes, A.E., Weinzierl, M.R., Donovan, F., and Noble, L.J. (2000). Vascular events after spinal cord injury: contribution to secondary pathogenesis. Phys. Ther. *80*, 673–687.

8. Silver, J., and Miller, J.H. (2004). Regeneration beyond the glial scar. Nat. Rev. Neurosci. *5*, 146–156. https://doi.org/10.1038/nrn1326.

9. Oyinbo, C.A. (2011). Secondary injury mechanisms in traumatic spinal cord injury: a nugget of this multiply cascade. Acta Neurobiol. Exp. *71*, 281–299.

10. Wang, X., Cao, K., Sun, X., Chen, Y., Duan, Z., Sun, L., Guo, L., Bai, P., Sun, D., Fan, J., et al. (2015). Macrophages in spinal cord injury: phenotypic and functional change from exposure to myelin debris. Glia *63*, 635–651. https://doi.org/10.1002/glia.22774.

11. Zhou, T., Zheng, Y., Sun, L., Badea, S.R., Jin, Y., Liu, Y., Rolfe, A.J., Sun, H., Wang, X., Cheng, Z., et al. (2019). Microvascular endothelial cells engulf myelin debris and promote macrophage recruitment and fibrosis after neural injury. Nat. Neurosci. *22*, 421–435. https://doi.org/10.1038/s41593-018-0324-9.

12. Wang, X., Cheng, Z., Tai, W., Shi, M., Ayazi, M., Liu, Y., Sun, L., Yu, C., Fan, Z., Guo, B., et al. (2024). Targeting foamy macrophages by manipulating ABCA1 expression to facilitate lesion healing in the injured spinal cord. Brain Behav. Immun. *119*, 431–453. https://doi.org/10.1016/j.bbi.2024.04.013.

13. Basso, D.M., Fisher, L.C., Anderson, A.J., Jakeman, L.B., McTigue, D.M., and Popovich, P.G. (2006). Basso Mouse Scale for locomotion detects differences in recovery after spinal cord injury in five common mouse strains. J. Neurotrauma *23*, 635–659. https://doi.org/10.1089/neu.2006.23.635.

14. Hoschouer, E.L., Finseth, T., Flinn, S., Basso, D.M., and Jakeman, L.B. (2010). Sensory stimulation prior to spinal cord injury induces post-injury dysesthesia in mice. J. Neurotrauma *27*, 777–787. https://doi.org/10.1089/neu.2009.1182.

15. Chen, J., Wu, Y., Duan, F.X., Wang, S.N., Guo, X.Y., Ding, S.Q., Zhou, J.H., Hu, J.G., and Lü, H.Z. (2019). Effect of M2 macrophage adoptive transfer on transcriptome profile of injured

spinal cords in rats. Exp. Biol. Med. *244*, 880–892. https://doi.org/10.1177/1535370219854668.

16. Nishi, R.A., Liu, H., Chu, Y., Hamamura, M., Su, M.Y., Nalcioglu, O., and Anderson, A.J. (2007). Behavioral, histological, and ex vivo magnetic resonance imaging assessment of graded contusion spinal cord injury in mice. J. Neurotrauma *24*, 674–689. https://doi.org/10.1089/neu.2006.0204.

17. Orr, M.B., Simkin, J., Bailey, W.M., Kadambi, N.S., McVicar, A.L., Veldhorst, A.K., and Gensel, J.C. (2017). Compression Decreases Anatomical and Functional Recovery and Alters Inflammation after Contusive Spinal Cord Injury. J. Neurotrauma *34*, 2342–2352. https://doi.org/10.1089/neu.2016.4915.

18. Harrison, M., O'Brien, A., Adams, L., Cowin, G., Ruitenberg, M.J., Sengul, G., and Watson, C. (2013). Vertebral landmarks for the identification of spinal cord segments in the mouse. Neuroimage *68*, 22–29. https://doi.org/10.1016/j.neuroimage.2012.11.048.

19. Ward, P.J., and Hubscher, C.H. (2012). Persistent polyuria in a rat spinal contusion model. J. Neurotrauma *29*, 2490–2498. https://doi.org/10.1089/neu.2012.2402.

20. Cummings, B.J., Engesser-Cesar, C., Cadena, G., and Anderson, A.J. (2007). Adaptation of a ladder beam walking task to assess locomotor recovery in mice following spinal cord injury. Behav. Brain Res. *177*, 232–241. https://doi.org/10.1016/j.bbr.2006.11.042.

21. Dolci, S., Pino, A., Berton, V., Gonzalez, P., Braga, A., Fumagalli, M., Bonfanti, E., Malpeli, G., Pari, F., Zorzin, S., et al. (2017). High Yield of Adult Oligodendrocyte Lineage Cells Obtained from Meningeal Biopsy. Front. Pharmacol. *8*, 703. https://doi.org/10.3389/fphar.2017.00703.